

ARTICLE

Vibrational Spectra and Adsorption of Trisiloxane Superspreading Surfactant at Air/Water Interface Studied with Sum Frequency Generation Vibrational Spectroscopy

Jun Feng^a, Dan Wu^{b†}, Jia Wen^{a‡}, Shi-lin Liu^a, Hong-fei Wang^{b*}

a. Hefei National Laboratory for Physical Sciences at Microscale, Department of Chemical Physics, University of Science and Technology of China, Hefei 230026, China

b. Beijing National Laboratory for Molecular Sciences, State Key Laboratory of Molecular Reaction Dynamics, Institute of Chemistry, Chinese Academy of Sciences, Beijing 100190, China

(Dated: Received on May 10, 2008; Accepted on Jun 6, 2008)

The C–H stretch vibrational spectra of the trisiloxane superspreading surfactant Silwet L-77 ((CH₃)₃Si–O–Si(CH₃)(C₃H₆)(OCH₂CH₂)_{7–8}OCH₃)–O–Si(CH₃)₃) at the air/water interface are measured with the surface Sum Frequency Generation Vibrational Spectroscopy (SFG-VS). The spectra are dominated with the features from the –Si–CH₃ groups around 2905 cm^{–1} (symmetric stretch or SS mode) and 2957 cm^{–1} (mostly the asymmetric stretch or AS mode), and with the weak but apparent contribution from the –O–CH₂– groups around 2880 cm^{–1} (symmetric stretch or SS mode). Comparison of the polarization dependent SFG spectra below and above the critical aggregate or micelle concentration (CAC) indicates that the molecular orientation of the C–H related molecular groups remained unchanged at different surface densities of the Silwet L-77 surfactant. The SFG-VS adsorption isotherm suggested that there was no sign of Silwet L-77 bilayer structure formation at the air/water interface. The Gibbs adsorption free energy of the Silwet surfactant to the air/water interface is –42.2±0.8 kcal/mol, indicating the unusually strong adsorption ability of the Silwet L-77 superspreading surfactant.

Key words: Trisiloxane surfactant, Superspreader, Surface adsorption, Sum frequency generation vibrational spectroscopy

I. INTRODUCTION

Superspreading is usually ascribed to the ability of the surfactant to decrease the surface tension of the aqueous spreading solution to as low as 20–21 mN/m, which is significantly lower than that of the solution with the conventional surfactant [1,2]. In the past decades, superspreading of the aqueous trisiloxane surfactant solutions over low-energy hydrophobic surfaces has attracted considerable interest because of its theoretical importance and practical applications [2–9]. Particularly, surfactants consisting of a relatively big trisiloxane hydrophobic headgroup (CH₃–Si(CH₃)₂–O–SiCH₃(CH₂)₃–O–Si(CH₃)₂–CH₃) and a polyethylene oxide polar group –(OCH₂CH₂)_n– (n=4–8) of four to eight units have the unique property to enable fast spreading of the aqueous solutions on various hydrophobic surfaces [2]. One of the com-

mercial trisiloxane superspreading surfactant that has been used as an effective wetting agents for water based herbicides on waxy plant leaves [10–12] and that has attracted tremendous theoretical interests is the Silwet L-77 with n=7 or 8 [2–9]. The molecular structure of the Silwet L-77 is shown in the Fig.1. In the literature, when n=8 and the end group is changed into –OH from

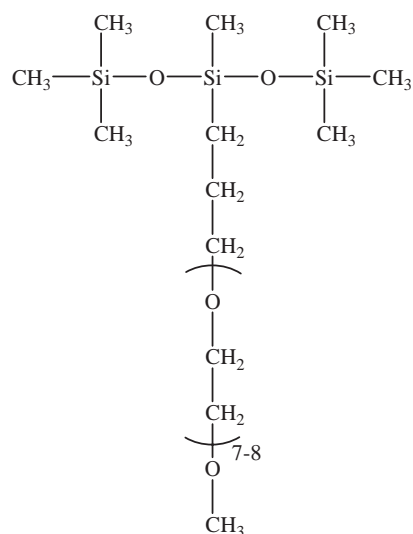


FIG. 1 Molecular structure of the trisiloxane surfactant Silwet L-77.

[†] Also graduate student of the Graduate University of the Chinese Academy of Sciences.

[‡] Undergraduate student in the Department of Chemical Physics, the University of Science and Technology of China. Current address: Department of Chemistry, University of California at Irvine, Irvine, CA 92697, U.S.A.

* Author to whom correspondence should be addressed. E-mail: hongfei@iccas.ac.cn, Tel.: +86-10-62555347, Fax: +86-10-62563167

–O–CH₃, the molecule is called TE₈ [13].

There have been different mechanisms proposed from experimental and theoretical studies on the superspreading phenomena of the trisiloxane surfactants. However, the molecular mechanism for the unique superspreading properties is yet to be fully understood. Experimental techniques, such as static and dynamic surface tension and contact angle measurement [1,14-21], real-time optical microscopy measurement of the spreading behavior on hydrophobic surfaces [5,21-23], infrared spectroscopy [13], neutron reflection [24], and solution phase behavior measurement [25], etc., and MD simulation [26,27] as well as theoretical modeling [28,29] were employed to probe and to understand the superspreading mechanism of the trisiloxane surfactants, particularly the Silwet L-77.

Among these studies, various structural models have been proposed for the Silwet L-77 molecule adsorbed at the water interface. For example, a dense bilayer model was derived from the surface tension [15], contact angle [16] and MD simulation [26] studies. It was also believed that the unique T shape of the trisiloxane head group for the Silwet L-77 molecule might favor the formation of the anti-parallel bilayer structure [26]. However, even though it is most certain that the T shaped molecular head group structure is one of the determining factors for the superspreading property for Silwet L-77, the chain length of the polyethylene oxide polar group –(OCH₂CH₂)_n– tail is also crucial. When $n < 4$ and $n > 8$, the superspreading ability of the trisiloxane molecule would be significantly reduced [1,17]. Besides the roles of the head group and the chain length of the tail of the surfactant molecule [1,17]. Recent studies also showed that the interactions between the adsorbed surfactant molecules and the interfacial water molecules may also play important roles [13]. Therefore, the detail knowledge of the structure and the interactions at the interface adsorbed with the superspreading surfactant can be very helpful in answering these questions.

In the past two decades, the surface sum frequency vibrational spectroscopy (SFG-VS) has been established as a powerful tool to study the molecular interfaces and films [30-37]. In SFG-VS, a visible laser beam is overlapped with an infrared (IR) beam at the interface to generate photons at the sum of the visible and IR laser frequencies. Because the SFG process is interface selective, the vibrational spectra of the interfacial molecular groups are obtained by tuning the frequency of the IR beam [30]. SFG-VS can provide the polarization dependent vibrational spectra of the various molecular groups at the interface for molecular orientation analysis. SFG-VS is especially powerful in studying the liquid interfaces, such as the water interfaces [37-39], where no other spectroscopic technique is capable of obtaining the detailed molecular information on the interfacial spectra, molecular orientation and interactions [35,36,40]. Recent developments in the quantitative interpretation of the polarization dependent SFG-

VS spectra have provided much detailed understanding of the molecular interfaces [36], especially on the accurate measurement of the spectral details [41-45], molecular orientation [45-48], as well as the determination of the double layer structure [49,50] of the polar adsorbate molecules at the interfaces.

These recent developments in the SFG-VS are particularly useful in order to answer the following two questions on the molecular structure and interactions at the superspreading surfactant adsorbed interfaces, namely, (i) whether there is a bilayer structure formed or not, and (ii) what are the structure and roles of the interfacial water molecules. To our knowledge, there has been no SFG-VS study on the superspreader interfaces so far. In this work, we shall use the SFG-VS to probe the C–H stretching vibrations of the Silwet L-77 molecule at the air/water interface in the spectral range of 2800-3000 cm⁻¹. We shall show from the SFG-VS adsorption isotherm of the C–H stretching vibrations that there was no sign of Silwet L-77 bilayer structure formation at the air/water interface. The studies on the interfacial water interaction with the adsorbed Silwet L-77 molecules shall be reported elsewhere.

II. THEORY OF SFG-VS

The principles of the SFG-VS theory for surface studies and data analysis have been well described in detail in the literatures [36,40]. The detailed formulation and procedures for quantitative calculation and simulation of the SFG-VS intensities or field strengths in different polarization combinations are also available [36,43]. Discussions on the interpretation of the SFG-VS spectral interference and the experimental configuration dependent SFG-VS spectra are available as well [44,45]. The empirical corrections of the bond additivity model (BAM) for quantitative interpretation of the SFG-VS spectra were also developed recently [51,52].

In summary, the SFG intensity $I(\omega)$ measured in a certain polarization combination and an experimental configuration from the interface region is a square function of the effective second order sum frequency susceptibility $\chi_{\text{eff}}^{(2)}$ [36,40]. In the reflective geometry, one has

$$I(\omega) = \frac{8\pi^3\omega^2\sec^2\beta}{c^3n_1(\omega)n_1(\omega_1)n_1(\omega_2)}|\chi_{\text{eff}}^{(2)}|^2I(\omega_1)I(\omega_2) \quad (1)$$

As defined previously [36], here c is the speed of the light in the vacuum; ω , ω_1 , and ω_2 are the frequencies of the SFG signal, visible, and IR laser beams, respectively; $n_j(\omega_i)$ is the refractive index of bulk medium j at frequency ω_i , and $n'(\omega_i)$ is the effective refractive index of the interface layer at ω_i . β_i is the incident or reflect angle from the interface normal of the i th light beam; $I(\omega_i)$ is the intensity of the SFG signal or the input laser beams.

In the single resonant SFG-VS, $\chi_{\text{eff}}^{(2)}$ depends on the infrared frequency ω_2 . One has,

$$\chi_{\text{eff}}^{(2)} = \chi_{\text{NR,eff}}^{(2)} + \sum_q \frac{\chi_{q,\text{eff}}^{(2)}}{\omega_2 - \omega_q + i\Gamma_q} \quad (2)$$

in which $\chi_{\text{NR,eff}}^{(2)}$ is the non-resonant contribution, and $\chi_{q,\text{eff}}^{(2)}$ (usually denote as $A_{q,\text{eff}}$) is the susceptibility (oscillator) strength factor for the q th vibrational mode in the SFG spectra centered at the vibrational frequency ω_q and with a damping constant Γ_q . Both $\chi_{\text{NR,eff}}^{(2)}$ and $\chi_{q,\text{eff}}^{(2)}$ are ensemble average values over molecules with different orientations. Because there are more than one vibrational mode ($q > 1$), the observed SFG-VS spectra are subject to the interference effects from the different vibrational modes. Such interference effects can be understood by fitting the observed SFG spectra with multiple modes following the Eq.(2). The relative values and the signs of the $\chi_{\text{NR,eff}}^{(2)}$ and $\chi_{q,\text{eff}}^{(2)}$ factors, as well as the spectral parameters ω_q and Γ_q , can be determined from spectral fittings of the SFG-VS spectra in different polarization combinations with different experimental configurations [38]. These values provide the spectral peak and intensity information which can be used to derive detailed information on the molecular orientation and interactions for the interfacial molecules.

The dependence of the $\chi_{q,\text{eff}}^{(2)}$ in different polarization combinations on the molecular orientation can be evaluated using the following unified functional form of molecular orientation [53,54]. The vibrational mode specific parameters c_q (general orientational parameter) and d_q (susceptibility strength factor) can be calculated for each vibrational mode according to its symmetry categories [36,38,43].

$$\begin{aligned} \chi_{q,\text{eff}}^{(2)} &= N_s \cdot d_q \cdot (\langle \cos \theta \rangle - c_q \cdot \langle \cos^3 \theta \rangle) \\ &= N_s \cdot d_q \cdot r_q(\theta) \end{aligned} \quad (3)$$

here $r_q(\theta)$ is the mode specific orientational field functional for the q th vibrational mode, which contains all molecular orientational information at a given SFG experimental configuration of that mode. The dimensionless parameter c_q for the q th vibrational mode determines the orientational response of $r_q(\theta)$ to the molecular tilt angle θ ; and d_q is the mode specific susceptibility strength factor for the q th vibrational mode, which is a constant for a certain experimental polarization combination. The d_q and c_q values are both functions of the related Fresnel coefficients including the refractive index of the interface and the bulk phases, the experimental geometry, and the symmetry of the q th vibrational mode. Examples on how to calculate the d_q and c_q values can be found [43].

Based on these formulations, the complex molecular orientation dependent interference effects between the different vibrational modes in different polarization

combinations can be simulated and quantitatively evaluated with the magnitude and phase (or sign) of the $d_q \cdot r_q(\theta)$ functional in each experimental configuration [44,45]. The simulation results and the evaluations can be directly compared with the SFG-VS experimental data in different polarization combinations under different experimental configurations. The symmetry properties of the vibrational modes and detailed orientational information of a particular molecular group at the interface can also be obtained accordingly [36,38,55].

The formulation in the Eq.(3) to separate the c_q and d_q terms is conceptually useful when the SFG-VS spectra under different experimental configurations and polarization combinations need to be compared [44,45]. In the SFG experiment, the xy plane in the laboratory coordinates system $\lambda(x, y, z)$ is generally defined as the plane of interface, with z as the interface normal; the p polarization is defined as the electric field vector within the xz plane, and the s polarization is the field vector perpendicular to the xz plane. The polarization combination ssp indicates that the fields of the SF signal, the visible beam, and the IR beam are in the s, s, and p polarizations, respectively; and so on. In general, there are four non-zero polarization combinations for a rotationally isotropic interface along the interface normal, namely, ssp, ppp, sps, and pss in the interface SFG-VS process. When doing experiment in different experimental configurations, i.e. with different visible and IR laser incident angles, the c_q values would remain unchanged for the ssp, sps, and pss polarization combinations, while the c_q value for the ppp would be very different. The d_q value for all q modes have the same scaling factors for the ssp, sps and pss polarization combinations, respectively; while the d_q value for the ppp is very different for each q mode, a result of the strong configuration dependence in the ppp polarization combination [44,45]. These are clearly illustrated previously [44,45], and also with the data for two different experimental configurations in this work.

III. EXPERIMENTS

A. Chemicals

The trisiloxane superspreading surfactant Silwet L-77 was purchased from the GE Chemicals and was used without further purification. Trisiloxane surfactant solutions were prepared using deionized water, which was the double distilled water purified and deionized with Millipore Simplicity 185 (18.2 M Ω cm). For all experiments the surfactant solutions were prepared within 48 h of testing in order to avoid potential hydrolytic degradation.

B. FTIR and Raman measurement

FTIR (BRUKER Tensor 27, resolution=4 cm $^{-1}$) and Raman (Bruker RFS-100, resolution=4 cm $^{-1}$) spectra

of the Silwet L-77 aqueous solutions were measured with the standard procedures.

C. SFG-VS measurement

The details of the SFG-VS experiment were described elsewhere [42]. Briefly, the 10 Hz and 23 picosecond SFG spectrometer laser system (EKSPLA) is in a co-propagating configuration. The wavelength of the visible light was set at 532 nm, and the full range of the IR wavelength was tunable from 1000-4300 cm^{-1} . The specified spectral resolution of this SFG spectrometer is $<6 \text{ cm}^{-1}$ in the whole IR range, and about 2 cm^{-1} around 3000 cm^{-1} . The energy of the visible beam was typically less than 300 μJ and that of the IR beam was less than 200 μJ . The spectra were first normalized to the intensities of the corresponding visible and IR laser pulses, and then normalized to the signal from Z-cut quartz. The detail of the normalization procedure followed the description [38]. The spectra were recorded by scanning the IR wavelength at 2 cm^{-1} increments, and each data point in the SFG spectra was an average of 300 laser pulses. All measurements were carried out at controlled room temperature ($22.0 \pm 1.0 \text{ }^\circ\text{C}$) and humidity ($50\% \pm 10\%$).

IV. RESULTS AND DISCUSSION

A. Interpretation of the SFG-VS spectra

Interpretation of the SFG-VS spectra of interfacial molecules used to rely on the interpretation and assignment of the IR and Raman spectra of the same molecules in the liquid, solid or even gaseous phases. However, recent SFG-VS studies have shown that on the one hand there are more SFG-VS spectral features can be identified for the molecules at the interface than those in the bulk phases with the IR and Raman, and on the other hand the intrinsically coherent and the polarization dependent nature of the SFG process allow new methodologies for spectral assignment and interpretation with the SFG-VS data. Firstly, a set of polarization selection rules was developed for the SFG-VS spectral assignment [36,42,43]; secondly, interference and experimental configuration analyses in the SFG-VS were developed to understand the overlapping features with multiple modes [44,45]. With the establishment of these methodologies, many new vibrational spectral features of the common molecules, such as simple alcohols and diols, were identified [36,42,43]. One of the interesting examples is with the C-H stretching vibrations of the ethanol molecules, whose new unexpected spectral features were determined with the SFG-VS studies at the interface. These assignments were then confirmed with very careful Raman and stimulated Raman measurements in the liquid and gaseous phases [41,45,56].

Using these ideas, the vibrational spectral of the Silwet L-77 in the C-H stretching vibration region can also be better understood.

The IR and Raman spectra of the Silwet L-77 in the Fig.2 shows three broad peaks at 2865, 2900, and 2960 cm^{-1} . The IR spectra of organosilicon compounds was first reported by Wright and Hunter in 1947 [57], and then summarized by Smith in 1960 [58]. According to these studies, the 2900 and 2960 cm^{-1} belong to the symmetric stretch (SS) and asymmetric stretch (AS) modes of the C-H vibrations of the -Si-CH₃ group, respectively. However, the assignment of the broad 2865 cm^{-1} band is much less explicit. It may contain the C-H stretching mode of both the -Si-CH₂- group [58], usually around 2860 cm^{-1} and the -(O-CH₂-CH₂)- group, usually around the 2870 and 2880 cm^{-1} [41,42].

In a recent FTIR study of the superspreader TE₈ molecules adsorbed on the OTS (octadecyltrichlorosilane) self-assembly monolayer (SAM) on the native oxide surface of silicon [13], four peaks were observed for the C-H stretching vibrations at the following wavelengths: 2880 and 2960 cm^{-1} , which were attributed to the SS and AS modes of the methyl groups in TE₈, respectively; and 2850 and 2920 cm^{-1} , which were attributed to the SS and AS modes of the methyl groups

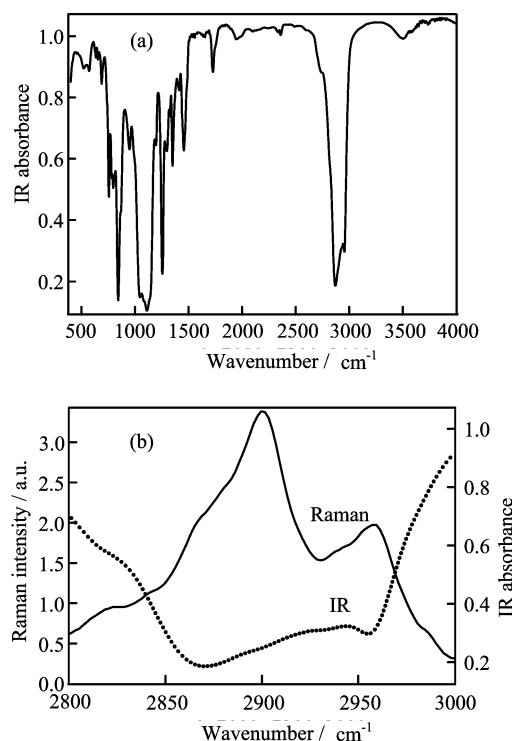


FIG. 2 FTIR and Raman spectra of the Silwet L-77. (a) the FTIR spectra in the range of 500-4000 cm^{-1} . (b) FTIR and Raman spectra. The spectral resolution of both the FTIR and Raman is 4 cm^{-1} . There are three broad band which can be identified around 2865, 2900, and 2960 cm^{-1} .

TABLE I Fitting results of the SFG spectra of the interface of the 91 $\mu\text{mol/L}$ Silwet L-77 aqueous solution in the following two experimental configurations. χ_{NR} is the non-resonant term.

Peak/ cm^{-1}	χ_{NR}	2879.7 \pm 1.6	2905.5 \pm 0.1	2957.6 \pm 0.1
Width (Γ_q)		10.2 \pm 1.5	9.6 \pm 0.2	5.6 \pm 0.1
Vis=45°, IR=52°	$A_{q,\text{ssp}}$	-0.021 \pm 0.001	0.47 \pm 0.08	-0.85 \pm 0.02
	$A_{q,\text{ppp}}$	0.009 \pm 0.002	0.27 \pm 0.08	-1.04 \pm 0.02
	$A_{q,\text{sps}}$	-0.004 \pm 0.003		0.40 \pm 0.02
Vis=63°, IR=50°	$A_{q,\text{ssp}}$	-0.019 \pm 0.001	0.28 \pm 0.06	-0.62 \pm 0.02
	$A_{q,\text{ppp}}$	0.032 \pm 0.002	0.03 \pm 0.05	-0.89 \pm 0.02

in TE_8 , respectively. Such spectra and assignment are not consistent with the IR and Raman spectra of the Silwet L-77 reported here. Furthermore, the assignment of the TE_8 spectra is also not reliable because it was based on the assignments of the n-alkyl carboxylic acid vibrational spectra [13,59], instead of on the assignment of the vibrational spectra of the organosilicon compounds as mentioned above [57,58].

We measured the SFG-VS spectra of the air/water interface of the Silwet L-77 aqueous solution at the 1.0 critical aggregate or micelle concentration (1.0 CAC = 91 $\mu\text{mol/L}$ for the TE_8) [13,17] taken in the following two experimental configurations with the visible and IR laser incident angles as: Vis=45°, IR=52°; and Vis=63°, IR=50°. We have not found the CAC value for the Silwet L-77 in the literature. Since it is believed that the CAC for TE_8 is with similar value for the Silwet L-77, here we used the CAC for the TE_8 to start preparing the Silwet L-77 solution. These SFG-VS spectra are shown in the Fig.3. The fitting results of these SFG-VS spectra are listed in the Table I. Here we found three peaks at 2879.7 \pm 1.6, 2905.5 \pm 0.1, and 2957.6 \pm 0.1 cm^{-1} , respectively.

According to the polarization selection rules in the SFG-VS [36,42,43], the 2879.7 and the 2905.5 cm^{-1} peaks are clearly SS modes, whose ssp intensity well exceed their ppp intensities; while the 2957.6 cm^{-1} peak is clearly a AS mode. To be in accordance with the previous literatures, we assigned the 2905.5 cm^{-1} peak and the 2957.6 cm^{-1} peak to the SS and AS modes of the $-\text{CH}_3$ group in the $-\text{Si}-\text{CH}_3$ groups of the Silwet L-77 molecule [36,42,43,57,58,60,61]; and the 2879.7 cm^{-1} peak to the SS mode of the $-\text{CH}_2-$ group in the $-\text{O}-\text{CH}_2-\text{CH}_2-$ units of the Silwet L-77 molecule [36,41,42,56]. The 2879.7 cm^{-1} peak does not belong to the SS mode of the $-\text{CH}_2-$ group in the $-\text{Si}-\text{CH}_2-\text{CH}_2-$ unit, because it was identified as around 2860 cm^{-1} [60], while the $-\text{CH}_2-$ group in the $-\text{O}-\text{CH}_2-$ unit is generally around 2880 cm^{-1} [36,41,42,56]. The ssp SFG intensity of the 2879.7 cm^{-1} peak is much smaller than those of the 2905.5 and the 2957.6 cm^{-1} peaks. This suggests that the 2879.7 cm^{-1} peak can not belong to the $-\text{CH}_3$ group in the $-\text{Si}-\text{CH}_3$ groups of the Silwet L-77 molecule. Other-

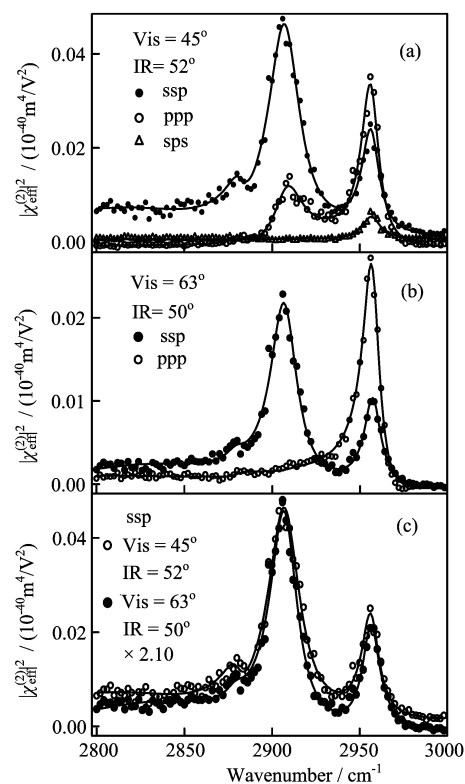


FIG. 3 SFG spectra of the air/liquid interface of the Silwet L-77 surfactant at 1.0 CAC in two different experimental configurations: (a) $\text{SF}_{2900\text{cm}^{-1}}=45.9^\circ$. (b) $\text{SF}_{2900\text{cm}^{-1}}=61.3^\circ$. The solid lines are the fitting results with Lorentzian line-shape functions. The fitting results are listed in the Table I. (c) Comparison of the $|\chi_{\text{eff}}^2|^2$ for the ssp polarization combinations in the two experimental configurations. According to the Eq.(1), here the scaling factor for the two experimental configuration at 2900 cm^{-1} is $\text{sec}^2 45.9 / \text{sec}^2 61.3 = 2.10$. Here the ssp spectra in the two experimental configurations are almost identical; while from the (a) and (b) panels, the ppp spectra are clearly different in the two experimental configurations.

wise its ssp SFG intensity must be stronger than that for the 2957.6 cm^{-1} peak [51,52]. The weak 2879.7 cm^{-1} peak intensity also indicates that the $-\text{O}-\text{CH}_2-\text{CH}_2-$ units of the Silwet L-77 molecules at the interface are

generally in an extend conformation, rather than a twisted or gauche conformation. Otherwise its SFG intensity should have been much stronger for that the number of the $-\text{O}-\text{CH}_2-\text{CH}_2-$ units is numerous. In IR or Raman, the intensity of the $-\text{CH}_2-$ group is generally dominant; while in the surface SFG-VS, only the gauche conformation of the chain gives comparable $-\text{CH}_2-$ group spectral intensity than that of the $-\text{CH}_3$ group [36,42], leaving the room for clear identification of the $-\text{CH}_3$ group features in the SFG spectra.

In order to further understand the SFG spectra of the interfacial Silwet L-77 molecules, the SFG spectra were taken in two different experimental configurations $\text{Vis}=45^\circ$, $\text{IR}=52^\circ$ and $\text{Vis}=63^\circ$, $\text{IR}=50^\circ$, as shown in the Fig.3. As expected [44,45], the Fig.3(c) shows that the ssp spectra in the two experimental configuration are almost identical with the expected scaling factor according to the Eq.(1).

On the other hand, the ppp SFG spectra of the two experimental configurations are significantly different. The 2905.5 cm^{-1} peak in the ppp spectrum in the $\text{Vis}=63^\circ$, $\text{IR}=50^\circ$ experimental configuration completely disappeared, while the 2957.6 cm^{-1} peak became relatively even stronger. There is only one 2957.6 cm^{-1} peak in the sps spectrum in the $\text{Vis}=45^\circ$, $\text{IR}=52^\circ$ configuration. These two facts clearly indicated that the 2957.6 cm^{-1} peak belongs to the AS mode of the $-\text{Si}-\text{CH}_3$ groups, and that the AS mode of the $-\text{CH}_2-$ groups is absent in the SFG spectra.

One prominent difference between the SFG-VS spectra for the two experimental configuration is that for the $\text{Vis}=63^\circ$, $\text{IR}=50^\circ$ configuration, the ppp 2957.6 cm^{-1} peak intensity is much higher than that of the ssp 2905.5 cm^{-1} peak intensity. In the $\text{Vis}=63^\circ$, $\text{IR}=50^\circ$ configuration, the relative SFG intensity of the 2957.6 cm^{-1} peak in the ppp and ssp polarization combinations is much larger than that of the $\text{Vis}=45^\circ$, $\text{IR}=52^\circ$ configuration. These are fully consistent with the simulations of the SS and AS modes of the $-\text{CH}_3$ group in different SFG-VS experimental configurations [45].

Further comparison of the polarization dependence of the 2905.5 and 2957.6 cm^{-1} peaks in the ssp, ppp, and sps polarization combinations also indicated that the 2957.6 cm^{-1} peak most likely contains contribution from the symmetric Fermi-resonance of the $-\text{CH}_2-$ group in the $-\text{O}-\text{CH}_2-$ unit, similar to what have been found for the ethanol and other alkyl alcohol molecules in their interfacial SFG-VS spectra [36,41,42,45,56]. From the fittings of the SFG-VS spectra in the $\text{Vis}=45^\circ$, $\text{IR}=52^\circ$ configuration in the Table I, one can get the following SFG intensity ratios: for the 2957.6 cm^{-1} peak, $I_{\text{ssp}}/I_{\text{ppp}}=A_{q,\text{ssp}}^2/A_{q,\text{ppp}}^2=0.67$, $I_{\text{sps}}/I_{\text{ppp}}=0.15$, and for the 2905.5 cm^{-1} peak, $I_{\text{ppp}}/I_{\text{ssp}}=0.21$. It has been known that for the AS mode of the C_{3v} groups, the relative SFG intensity depends on the interfacial microscopic local field factors at the visible and SF frequency, i.e. the effective interfacial refractive index n' ;

while that of its SS mode depends on both the n' and the molecular polarizability depolarization ratio R [36]. Since here both n' and R are not known *a priori*, we simulated the above intensity ratios by varying the n' values for the AS mode, and by varying the n' values with differences for the SS mode. The simulation results is shown in the Fig.4. here, for the SS mode simulation, only the $R=3.4$, which is typical for the alkyl $-\text{CH}_3$ groups, results are plotted.

From the Fig.4, one can find that in order to satisfy the $I_{\text{ssp}}/I_{\text{ppp}}=0.67$ and $I_{\text{sps}}/I_{\text{ppp}}=0.15$ ratios for the AS mode (i.e. the 2957.6 cm^{-1} peak), n' has to be above 1.50 and the average tilt angle of the $-\text{CH}_3$ group has to be around 53° . However, this n' value and the average tilt angle value would make it impossible to satisfy the experimental $I_{\text{ppp}}/I_{\text{ssp}}=0.21$ value for the SS mode (i.e. the 2905.5 cm^{-1} peak) even the R value is changed in the full allowed range between 1.0 and 4.0 [36,40]. In addition, it is also not likely to have $n'=1.50$, since it is a somewhat unexpectedly high value for the interfacial effective refractive index [36,40]. Through Raman and SFG-VS isotope substitutions, as

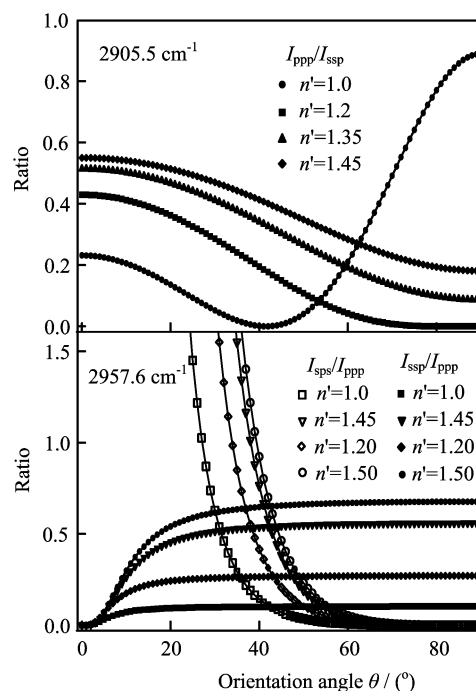


FIG. 4 Simulation of the SFG intensity ratios for the $-\text{Si}-\text{CH}_3$ SS and $-\text{Si}-\text{CH}_3$ AS mode in the experimental configuration $\text{Vis}=45^\circ$, $\text{IR}=52^\circ$ against the average tilt angle of the $-\text{Si}-\text{CH}_3$ group using different effective interfacial refractive index n' values. Because there are seven $-\text{Si}-\text{CH}_3$ groups in each Silwet L-77 molecule, it is not meaningful to discuss the tilt angle of each individual $-\text{Si}-\text{CH}_3$ group. It is clear that the SS and AS modes have very different sensitivities to the n' value. The simulation results indicate that the 2957.6 cm^{-1} peak may contain contribution from the $-\text{O}-\text{CH}_2-\text{CH}_2$ SS C-H Fermi resonance mode. See main text.

TABLE II Fitting results of the SFG spectra at various bulk concentrations using the units of 1.0 CAC=91 $\mu\text{mol/L}$ in the experimental configuration of $\text{Vis}=45^\circ$, $\text{IR}=55^\circ$. χ_{NR} is the non-resonant term. This CAC concentration is for the TE_8 solution. The actual CAC of the Silwet L-77 aqueous solution is somewhat smaller.

Peak/ cm^{-1}		χ_{NR}	2875.8 \pm 1.2	2903.5 \pm 0.1	2957.6 \pm 0.1
Width (Γ_q)			9.2 \pm 0.8	9.9 \pm 0.1	6.9 \pm 0.1
5.0 CAC	$A_{q,\text{ssp}}$	-0.035 \pm 0.001	0.29 \pm 0.02	2.13 \pm 0.02	-1.21 \pm 0.02
	$A_{q,\text{ppp}}$	0.003 \pm 0.001	0.25 \pm 0.05	1.03 \pm 0.02	-1.23 \pm 0.02
	$A_{q,\text{sps}}$	-0.019 \pm 0.002			0.56 \pm 0.02
1.0 CAC	$A_{q,\text{ssp}}$	-0.031 \pm 0.001	0.21 \pm 0.02	2.09 \pm 0.02	-1.22 \pm 0.02
	$A_{q,\text{ppp}}$	0.003 \pm 0.001	0.28 \pm 0.05	0.97 \pm 0.02	-1.23 \pm 0.02
	$A_{q,\text{sps}}$	-0.018 \pm 0.002			0.56 \pm 0.02
0.25 CAC	$A_{q,\text{ssp}}$	-0.033 \pm 0.001	0.27 \pm 0.02	1.90 \pm 0.02	-1.13 \pm 0.02
	$A_{q,\text{ppp}}$	0.002 \pm 0.001	0.26 \pm 0.05	0.89 \pm 0.03	-1.16 \pm 0.02
	$A_{q,\text{sps}}$	-0.015 \pm 0.003			0.53 \pm 0.02
0.05 CAC	$A_{q,\text{ssp}}$	-0.025 \pm 0.001	0.36 \pm 0.03	1.46 \pm 0.02	-0.88 \pm 0.02
	$A_{q,\text{ppp}}$	0.003 \pm 0.001	0.17 \pm 0.08	0.60 \pm 0.03	-0.95 \pm 0.02
	$A_{q,\text{sps}}$	-0.011 \pm 0.004			0.36 \pm 0.03
0.01 CAC	$A_{q,\text{ssp}}$	-0.024 \pm 0.002	0.39 \pm 0.03	0.65 \pm 0.03	-0.45 \pm 0.03
	$A_{q,\text{ppp}}$	0.008 \pm 0.003	-0.26 \pm 0.08	0.23 \pm 0.10	-0.47 \pm 0.02
	$A_{q,\text{sps}}$	-0.007 \pm 0.002			0.09 \pm 0.04

well as the SFG-VS experimental configuration analysis [36,41,42,45,56], it has been well established that the AS mode of the $-\text{CH}_3$ group in the ethanol and alkyl alcohol molecules around the 2960 cm^{-1} contains contribution from the Fermi resonance mode of the $-\text{CH}_2-$ groups or the $-\text{O}-\text{CH}_2-$ groups. Here, we surmise that even though the 2957.6 cm^{-1} peak is dominated by the AS C-H mode of the $-\text{Si}-\text{CH}_3$ groups, it also contains contributions from the Fermi-resonance SS C-H mode of the $-\text{O}-\text{CH}_2-\text{CH}_2-$ units.

B. Silwet L-77 adsorption isotherm and structure at the air/water interface

The SFG-VS adsorption isotherm of the Silwet L-77 at the air/water interface can provide the information of the adsorption structure and thermodynamic parameter of the adsorption process. Figure 5 presents the SFG data for the air/water interface of the Silwet L-77 aqueous solutions at the following concentrations, 0.01, 0.05, 0.25, 1.0, and 5.0 CAC, with the experimental configuration of $\text{Vis}=45^\circ$, $\text{IR}=55^\circ$. The SFG spectra at 1.0 CAC is very close to the 1.0 CAC data obtained with the $\text{Vis}=45^\circ$, $\text{IR}=52^\circ$, since the SFG spectra are more sensitive to the incident angle of the visible beam and much less sensitive to the incident angle of the IR beam [38,39,48]. The fitting parameters of the data in the Fig.5 are listed in the Table II. The three peak positions are at 2875.8 \pm 1.2, 2903.5 \pm 0.1, and 2957.6 \pm 0.1 cm^{-1} , respectively. They are consistent with the peak positions as obtained from the $\text{Vis}=45^\circ$, $\text{IR}=52^\circ$ and $\text{Vis}=63^\circ$, $\text{IR}=50^\circ$ experimental configura-

tions.

Figure 6 plots the ratios of the $A_{q,\text{ssp}}/A_{q,\text{ppp}}$ for the 2903.5 and the 2957.6 cm^{-1} peaks at the five bulk concentrations. The Eq.(3) indicates that the $A_{q,\text{ssp}}/A_{q,\text{ppp}}$ ratio is independent from the surface number density and dependent on the molecular orientation functions [62]. Here in the Fig.6 both ratios remained unchanged within the experimental error, indicating that the average tilt of the $-\text{Si}-\text{CH}_3$ groups remained unchanged as the bulk Silwet L-77 concentration increased. Thus, the average orientation of the Silwet L-77 molecules adsorbed at the air/water interface also remained unchanged.

Figure 7 plots the SFG-VS Langmuir adsorption isotherm, i.e. $A_{q,ijk}$ vs. bulk concentration, of all the five peaks in the ssp, ppp, and sps polarization combinations. It is clear that all five isotherm followed the single layer Langmuir isotherm, instead of the anti-parallel double layer Langmuir isotherm, where a drop of the total SFG-VS oscillator strength $A_{q,ijk}$ at the higher bulk concentration than the saturation bulk concentration is expected [49,50]. Such anti-parallel were identified for the adsorbed layers of the various simple dipolar organic molecules, such as methanol and acetone, at the air/water interface using the SFG-VS adsorption isotherm and orientation analysis [49,50]. Following the same lines in these works [49,50], the results here clearly indicated that the picture of an anti-parallel bilayer layer structure of the Silwet L-77 as suggested by some previous studies is not the case [16,26].

The Langmuir isotherms in the Fig.7 indicate that the CAC for the Silwet L-77 is actually around 0.25 CAC

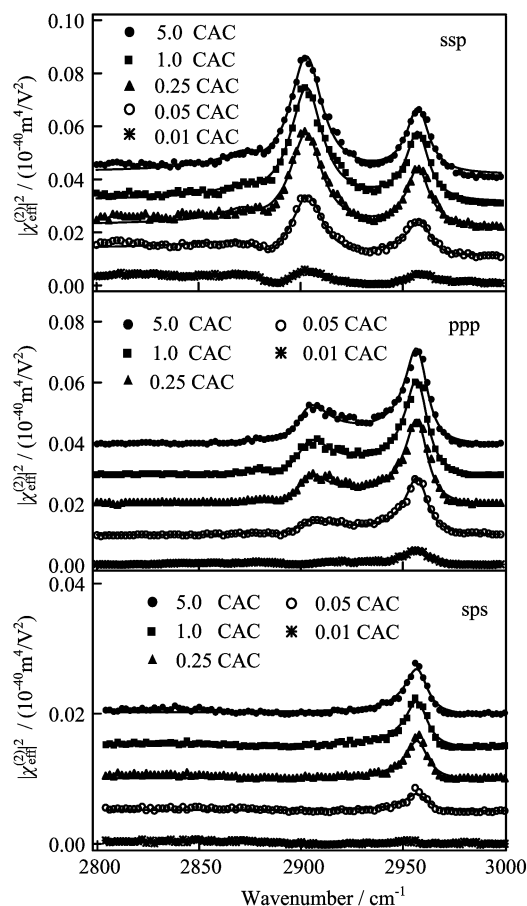


FIG. 5 The C–H stretching vibrational spectra of the trisiloxane surfactant in the polarization combinations of ssp, ppp, and sps at the bulk mixture concentration of 0.01, 0.05, 0.25, 1.0, and 5.0 CAC. The experimental configuration is $\text{Vis}=45^\circ$ and $\text{IR}=55^\circ$. The solid lines are the fitting results with Lorentzian line-shape functions. The fitting results are listed in the Table II.

of the TE_8 , pointing to stronger adsorption ability to the air/water interface for the Silwet L-77 than that of the TE_8 . Fitting of the Langmuir adsorption isotherms with the simple Langmuir model gives the adsorption free energy of the Silwet L-77 to the air/water interface [63]. Because $A_{q,ijk}$ is proportional to the surface number density N_s , one has

$$\frac{A_{q,ijk}}{A_{q,ijk}^{\max}} = \frac{1}{1 + 55.55/KC} \quad (4)$$

here 55.55 is the concentration of the water molecule in the solution, C is the Silwet L-77 bulk concentration, K is the adsorption equilibrium constant, $A_{q,ijk}^{\max}$ is the maximum oscillator strength of a full monolayer. Fitting of the Langmuir isotherm, i.e. $A_{q,ijk}$ vs. C curves, is carried out with K and $A_{q,ijk}^{\max}$ as fitting parameters. The adsorption free energy is obtained through $\Delta G_{\text{ads}}^\circ = -RT \ln K$. Since the five isotherms reach saturation at very similar bulk concentrations, their K and $\Delta G_{\text{ads}}^\circ$ are very close to each other.

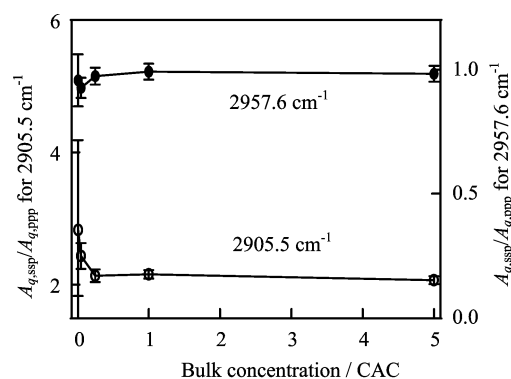


FIG. 6 $A_{q,\text{ssp}}/A_{q,\text{ppp}}$ ratio vs. trisiloxane surfactant concentration for the $-\text{Si}-\text{CH}_3$ SS (2905.5 cm^{-1}) and $-\text{Si}-\text{CH}_3$ AS (2957.6 cm^{-1}) modes. These results indicated that the averaged orientation of the $-\text{Si}-\text{CH}_3$ group remained almost unchanged in the broad range of surfactant concentration.

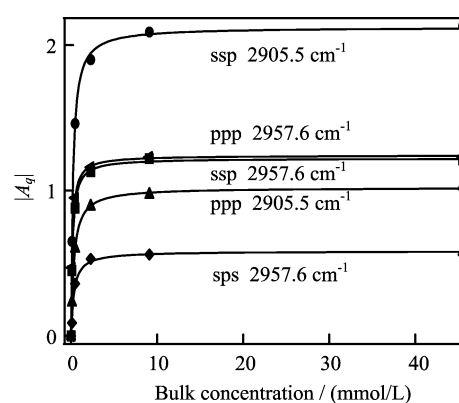


FIG. 7 $|A_q|$ of the five spectral peaks in the ssp, ppp, and sps spectra as a function of the bulk trisiloxane surfactant concentration. Since all $|A_q|$ curves saturate at high concentration, there is no sign of the Silwet L-77 bilayer structure formation. All these curves yielded very similar adsorption free energy for the Silwet L-77 adsorption to the air/water interface. The solid lines are the fitting results with the Eq.(4).

A global fitting gives $K=(2.8\pm 0.8)\times 10^7$ and $\Delta G_{\text{ads}}^\circ = -42.2\pm 0.8 \text{ kJ/mol}$. The adsorption free energy indicates a very strong adsorption of the Silwet L-77 to the air/water interface. It is slightly smaller than the values for the Silwet L-77 adsorption to the air/water interface of the phosphate buffer solution in Ref.[1].

V. CONCLUSION

The CH stretching vibrational spectra of the trisiloxane superspreading surfactant Silwet L-77 were studied using FTIR, Raman, and surface sum frequency vibrational spectroscopy. The SFG-VS spectra at the air/water interface were dominated with the features

from the $-\text{Si}-\text{CH}_3$ groups around 2905 cm^{-1} (symmetric stretch or SS mode) and 2957 cm^{-1} (mostly the asymmetric stretch or AS mode), and with the weak but apparent contribution from the $-\text{O}-\text{CH}_2-$ groups around 2880 cm^{-1} (symmetric stretch or SS mode). Comparison of the polarization dependent SFG spectra below and above the CAC (Critical aggregate concentration) indicated that the molecular orientation of the C-H related molecular groups remained almost unchanged at different surface densities of the Silwet L-77 surfactant. The SFG-VS adsorption isotherm suggested that there was no sign of Silwet L-77 bilayer structure formation at the air/water interface. The adsorption free energy of the Silwet L-77 surfactant to the air/water interface was $-42.2 \pm 0.8\text{ kJ/mol}$, indicating unusually strong adsorption ability of the Silwet L-77 superspreading surfactant to the air/water interface.

It is so far the first study of the interfacial trisiloxane surfactants with the interface selective SFG-VS technique. Even though the results presented in this study still can not solve the mechanism for the superspreading phenomena of the trisiloxane surfactants, it provided strong and direct experimental evidences to conclude that there is no sign of anti-parallel bilayer structure formation at the air/water interface [16,26]. We also presented the analysis and assignment of the vibrational spectral features of the Silwet L-77 molecules adsorbed at the air/water interface. These results suggested that the structure of the surfactant alone may not be able to provide solution to the superspreading mechanism. Therefore, the structure and interaction of the interfacial water molecules at the trisiloxane surfactant solution interface must have important roles. We shall report the SFG-VS results on the interfacial water molecules at the Silwet L-77 solution interfaces in the near future.

VI. ACKNOWLEDGEMENTS

Jun Feng thanks the helpful discussion from Ganghua Deng and Yuan Wang. Hong-fei Wang thanks Dr. Wen-qing Peng at the GE China Technology Center (CTC) in Shanghai for bringing his attention to the superspreading phenomenon during his visit at GE CTC in November 2006. Hong-fei Wang thanks the support by the National Natural Science Foundation of China (No.20425309 and No.20533070) and the Ministry of Science and Technology of China (No.2007CB815205). Shi-lin Liu thanks the support by the National Natural Science Foundation of China (No.20533070).

- [1] M. J. Rosen and Y. F. Wu, *Langmuir* **17**, 7296 (2001).
- [2] R. M. Hill, *Curr. Opin. Coll. Inter. Sci.* **3**, 247 (1998).
- [3] Z. Lin, R. M. Hill, H. T. Davis, and M. D. Ward, *Langmuir* **10**, 4060 (1994).

- [4] T. F. Svitova, H. Hoffmann, and R. M. Hill, *Langmuir* **12**, 1712 (1996).
- [5] T. Stoebe, Z. Lin, R. M. Hill, M. D. Ward, and H. T. Davis, *Langmuir* **13**, 7270 (1997).
- [6] T. Stoebe, Z. Lin, R. M. Hill, M. D. Ward, and H. T. Davis, *Langmuir* **13**, 7276 (1997).
- [7] T. Stoebe, Z. Lin, R. M. Hill, M. D. Ward, and H. T. Davis, *Langmuir* **13**, 7282 (1997).
- [8] T. F. Svitova, R. M. Hill and C. J. Radke, *Langmuir* **17**, 335 (2001).
- [9] T. F. Svitova, Y. P. Smirnova, and G. Yakubov, *Coll. Surf.* **101**, 251 (1995).
- [10] J. A. Zabkiewicz and R. E. Gaskin, *Adjuvants Agrochem.* **1**, 141 (1989).
- [11] R. E. Gaskin and R. C. Kirkwood, *Adjuvants Agrochem.* **1**, 129 (1989).
- [12] M. Knoche, H. Tamura, and M. Bukovac, *J. Agric. Food Chem.* **39**, 202 (1991).
- [13] N. Kumar, C. Maldarelli, and A. Couzis, *Coll. Surf. A* **277**, 98 (2006).
- [14] M. von Bahr, F. Tiberg, and B. V. Zhmud, *Langmuir* **15**, 7069 (1999).
- [15] J. Venzmer and S. P. Wilkowski, *Pesticides Formulations and Application Systems* **18**, 1347 (1998).
- [16] F. Tiberg and A. M. Cazabat, *Langmuir* **10**, 2301 (1994).
- [17] N. Kumar, A. Couzis and C. Maldarelli, *J. Coll. Inter. Sci.* **267**, 272 (2003).
- [18] K. P. Ananthapadmanabhan, E. D. Goddard, and P. Chandra, *Coll. Surf. A* **44**, 281 (1990).
- [19] Y. F. Wu and M. J. Rosen, *Langmuir* **18**, 2205 (2002).
- [20] S. Rafai, D. Sarker, V. Bergeron, J. Meunier, and D. Bonn, *Langmuir* **18**, 10486 (2002).
- [21] S. Zhu, W. G. Miller, L. E. Striven, and H. T. Davis, *Coll. Surf. A* **90**, 63 (1994).
- [22] M. He, R. M. Hill, Z. Liu, L. E. Scieven, and H. T. Davis, *J. Phys. Chem.* **97**, 8820 (1993).
- [23] A. D. Nikolov, D. T. Wasan, A. Chengara, K. Koczko, G. A. Policello, and I. Kolossvary, *Adv. Coll. Interface Sci.* **96**, 325 (2002).
- [24] J. R. Lu, Z. X. Li, R. K. Thomas, B. P. Bink, D. Crichton, P. D. L. Fletcher, J. R. McNab, and J. Penfold, *J. Phys. Chem. B* **102**, 5785 (1998).
- [25] H. Kunieda, H. Taoka, T. Iwanaga, and A. Harashima, *Langmuir* **14**, 5113 (1998).
- [26] Y. Y. Shen, A. Couzis, J. Koplik, C. Maldarelli, and M. S. Tomassone, *Langmuir* **21**, 12160 (2005).
- [27] H. Y. Kim, Y. Qin, and K. A. Fichthorn, *J. Chem. Phys.* **125**, 174708 (2006).
- [28] A. Kabalnov, *Langmuir* **16**, 2595 (2000).
- [29] A. Kabalnov, *Eur. Phys. J. E.* **2**, 255 (2000).
- [30] Y. R. Shen, *Nature* **337**, 519 (1989).
- [31] K. B. Eisenthal, *Chem. Rev.* **96**, 1343 (1996).
- [32] C. D. Bain, *J. Chem. Soc. Faraday Trans.* **91**, 1281 (1995).
- [33] M. J. Shultz, C. Schnitzer, and S. Baldelli, *Int. Rev. Phys. Chem.* **19**, 123 (2000).
- [34] G. L. Richmond, *Chem. Rev.* **102**, 2693 (2002).
- [35] P. B. Miranda and Y. R. Shen, *J. Phys. Chem. B* **103**, 3292 (1999).
- [36] H. F. Wang, W. Gan, R. Lu, Y. Rao, and B. H. Wu, *Int. Rev. Phys. Chem.* **24**, 191 (2005).
- [37] Y. R. Shen and V. Ostroverkhov, *Chem. Rev.* **106**, 1140

- (2006).
- [38] W. Gan, D. Wu, Z. Zhang, and H. F. Wang, *J. Chem. Phys.* **124**, 114705 (2006).
- [39] W. Gan, D. Wu, Z. Zhang, Y. Guo, and H. F. Wang, *Chin. J. Chem. Phys.* **19**, 20 (2006)
- [40] X. W. Zhuang, P. B. Miranda, D. Kim, and Y. R. Shen, *Phys. Rev. B* **59**, 12632 (1999).
- [41] W. Gan, Z. Zhang, R. R. Feng, and H. F. Wang, *Chem. Phys. Lett.* **423**, 261 (2006).
- [42] R. Lu, W. Gan, B. H. Wu, H. Chen, and H. F. Wang, *J. Phys. Chem. B* **108**, 7297 (2004).
- [43] R. Lu, W. Gan, B. H. Wu, Z. Zhang, Y. Guo, and H. F. Wang, *J. Phys. Chem. B* **109**, 14118 (2005).
- [44] W. Gan, B. H. Wu, Z. Zhang, Y. Guo, and H. F. Wang, *J. Phys. Chem. C* **111**, 8716 (2007).
- [45] W. Gan, Z. Zhang, R. R. Feng, and H. F. Wang, *J. Phys. Chem. C* **111**, 8726 (2007).
- [46] H. Chen, W. Gan, B. H. Wu, D. Wu, Z. Zhang, and H. F. Wang, *Chem. Phys. Lett.* **408**, 284 (2005).
- [47] (a) R. Lu, W. Gan, and H. F. Wang, *Chin. Sci. Bull.* **48**, 2183 (2003).
(b) R. Lu, W. Gan, and H. F. Wang, *Chin. Sci. Bull.* **49**, 899 (2004).
- [48] W. Gan, B. H. Wu, H. Chen, Y. Guo, and H. F. Wang, *Chem. Phys. Lett.* **406**, 467 (2005).
- [49] H. Chen, W. Gan, B. H. Wu, D. Wu, Y. Guo, and H. F. Wang, *J. Phys. Chem. B* **109**, 8053 (2005).
- [50] H. Chen, W. Gan, R. Lu, Y. Guo, and H. F. Wang, *J. Phys. Chem. B* **109**, 8064 (2005).
- [51] H. Wu, W. K. Zhang, W. Gan, Z. F. Cui, and H. F. Wang, *J. Chem. Phys.* **125**, 133203 (2006).
- [52] H. Wu, W. K. Zhang, W. Gan, Z. F. Cui, and H. F. Wang, *Chin. J. Chem. Phys.* **19**, 187 (2006).
- [53] H. F. Wang, *Chin. J. Chem. Phys.* **17**, 362 (2004).
- [54] Y. Rao, Y. S. Tao, and H. F. Wang, *J. Chem. Phys.* **119**, 5226 (2003).
- [55] W. Gan, D. Wu, Z. Zhang, and H. F. Wang, *Chin. J. Chem. Phys.* **19**, 20 (2006).
- [56] Y. Q. Yu, K. Lin, X. G. Zhou, H. F. Wang, S. L. Liu, and X. X. Ma, *J. Phys. Chem. C* **111**, 8971 (2007).
- [57] N. Wright and M. J. Hunter, *J. Am. Chem. Soc.* **69**, 803 (1947)
- [58] A. L. Smith, *Spectrochim. Acta* **16**, 87 (1960)
- [59] I. R. Hill and I. W. Levin, *J. Chem. Phys.* **70**, 842 (1979).
- [60] C. Y. Chen, J. Wang, and Z. Chen, *Langmuir* **20**, 10186 (2004).
- [61] H. K. Ye, Z. Y. Gu, and D. H. Gracias, *Langmuir* **22**, 1863 (2006).
- [62] J. Sung, K. Park, and D. Kim, *J. Phys. Chem. B* **109**, 18507 (2005).
- [63] H. F. Wang, E. C. Y. Yan, Y. Liu, and K. B. Eisenthal, *J. Phys. Chem. B* **102**, 4446 (1998).